

RESEARCH ARTICLE

Elongated mitochondrial constrictions and fission in muscle fatigue

Manuela Lavorato^{1,2,*}, Emanuele Loro³, Valentina Debattisti⁴, Tejvir S. Khurana³ and Clara Franzini-Armstrong¹

ABSTRACT

Mitochondria respond to stress and undergo fusion and fission at variable rates, depending on cell status. To understand mitochondrial behavior during muscle fatigue, we investigated mitochondrial ultrastructure and expression levels of a fission- and stress-related protein in fast-twitch muscle fibers of mice subjected to fatigue testing. Mice were subjected to running at increasing speed until exhaustion at 45 min–1 h. In further experiments, high-intensity muscle stimulation through the sciatic nerve simulated the forced treadmill exercise. We detected a rare phenotype characterized by elongated mitochondrial constrictions (EMCs) connecting two separate segments of the original organelles. EMCs are rare in resting muscles and their frequency increases, albeit still at low levels, in stimulated muscles. The constrictions are accompanied by elevated phosphorylation of Drp1 (Dnm1l) at Ser 616, indicating an increased translocation of Drp1 to the mitochondrial membrane. This is indicative of a mitochondrial stress response, perhaps leading to or facilitating a long-lasting fission event. A close apposition of sarcoplasmic reticulum (SR) to the constricted areas, detected using both transmission and scanning electron microscopy, is highly suggestive of SR involvement in inducing mitochondrial constrictions.

KEY WORDS: Fatigue, Fission, Mitochondria, Skeletal muscle

INTRODUCTION

Mitochondria, the cells' permanent guests, are very dynamic and extremely sensitive to their environment. They mostly have specific intracellular distributions that can directly contribute to the control of calcium homeostasis within differentiated cells (Tinel et al., 1999). Their precise positioning is at least in part due to small tethers that ensure association of the organelles with elements of the endoplasmic reticulum (ER) (Mannella et al., 1998) and of the sarcoplasmic reticulum (SR) in muscle (Boncompagni et al., 2009b). Mitochondrial fission and fusion events, which are important during and immediately after cell division, also occur continually in interphase cells and are of primary importance in maintaining mitochondrial size and shape as well as, indirectly, cellular homeostasis and general health of the organism (Chen and Chan, 2010; Westermann, 2010; Chan, 2012; Rana et al., 2017).

Mitochondria are particularly sensitive to the cytoplasmic milieu; they are directly affected by changes in the concentration of various cytoplasmic components, resulting in variations of their density, positioning and ultrastructure. Structural mitochondrial modulations are easily induced in muscle. For example, even an acute exercise of short duration may affect specific inter-mitochondrial connections modulated by their surface membrane (Picard et al., 2013), and fragmentation can be induced by cardiac exercise (Coronado et al., 2018). Long-range effects occur in myopathies affecting calcium homeostasis, such as central core disease and malignant hyperthermia in which mitochondrial morphology, distribution and fragmentation are strongly affected (Boncompagni et al., 2009b; Lavorato et al., 2016). Prolonged unbalanced Ca^{2+} homeostasis in the myocardium activates the fission process, resulting in increased frequency of mitochondrial profiles due to fragmentation, while also inducing prolonged nanotunneling extensions in the usually structurally conservative cardiac mitochondria (Lavorato et al., 2015, 2017).

Striated muscles (skeletal and cardiac) are particularly appropriate subjects for the detection of subtle alterations in mitochondrial ultrastructure, positioning and frequency, because the organelles have a highly stereotyped, developmentally regulated, cell type-specific distribution in relationship to other cell components (Boncompagni et al., 2009a). Additionally, controlled alterations in cytoplasmic composition can be easily induced by subjecting the muscles to exercise and monitoring the induced fatigue. The term fatigue is generally used to indicate a complex alteration in muscle status in which the contraction response to a given stimulus is reduced in strength. It is not an absolute term, it involves intermediate stages in which muscle can still operate although at reduced power output levels, as well as terminal stages where no force is produced. Fatigue results from a combination of causes, mostly at the level of the muscle fiber itself, even in experimental *in vivo* setups that involve contributions from respiratory and cardiovascular systems, nerve conduction and synaptic transmission (Fitt, 1994). Fatigue is a complex phenomenon, involving profound alterations in the cytoplasmic milieu (extensively reviewed by Fitt, 1994). For example, despite the cell's complex metabolic system that has evolved in order to ensure relatively constant ATP levels, loss of ATP, accumulation of ADP and general acidification of the cytoplasm accompany fatigue-inducing exercise (Westerblad and Allen, 1992, 1993). Additionally, changes in Mg levels (Westerblad and Allen, 1992; Nassar-Gentina et al., 1981), accumulation of lactate from glycolysis and of inorganic phosphate from breakdown of creatine phosphate (Allen and Westerblad, 2001), and in more extreme cases, changes in the rate of ATP hydrolysis (Nagasser et al., 1992) and reduction or failure to release calcium (Westerblad and Allen, 1993) can occur. Production and accumulation of active oxygen species has been more recently added to the list of fatigue-related alterations (Cheng et al., 2016; Kamandulis et al., 2017). Oxygen demand is also altered during strong exercise; it may

¹Department of Cell and Developmental Biology, University of Pennsylvania, Philadelphia, PA 19104, USA. ²Department of Genetics, Children's Hospital of Philadelphia, PA 19104, USA. ³Department of Physiology, University of Pennsylvania, Philadelphia, PA 19104, USA. ⁴MitoCare Center, Department of Pathology, Anatomy, and Cell Biology, Thomas Jefferson University, Philadelphia, PA 19107, USA.

*Author for correspondence (manuelalavorato@gmail.com)

© M.L., 0000-0001-6170-259X; E.L., 0000-0002-0822-4514

increase more than 20-fold in human skeletal muscle during intense exercise (Bangsbo, 2000).

The aim of this study was to detect ultrastructural alterations in mitochondria resulting from exercise and/or direct electrical stimulation that induced some level of fatigue. Fatigue was detected by faltering in treadmill-exercised mice and by a reduction in recorded force response in electrically stimulated muscles. Both indicated an alteration in the cytoplasmic milieu that was likely to affect mitochondria. In order to investigate the accelerated effect of the stimulation, we focused our analysis on the fibers most prone to fatigue – the fast-twitch type IIB/IIX fibers. We discovered a novel structural modification of mitochondria with the appearance of elongated constrictions closely associated with SR elements. These may be indicative of a stress response and possibly of initial fission stages. The imaging was facilitated by the highly organized disposition of mitochondria in mouse skeletal muscle, which is rich in organized mitochondrial networks with complex interconnections (Franzini-Armstrong, 2007; Franzini-Armstrong and Boncompagni, 2011; Dahl et al., 2015; Glancy et al., 2015). In confirmation of the structural data we detected a fatigue-related increase in the phosphorylation of Drp1 (also known as Dnm11) at Ser 616, a change that has been associated with the translocation of Drp1 to the mitochondrial membrane, indicating a stress response of the mitochondria (Wei et al., 2011; Zhang et al., 2017) and possibly leading to the fission process (Taguchi et al., 2007).

RESULTS

Average mitochondrial width is reduced and frequency of elongated mitochondrial constrictions is higher in fibers from exercise-fatigued mice

The large majority of mitochondria in cross-sectional areas of IIB/IIX fibers appear as thin elongated cylinders, oriented with their long axis in the transverse plane and located at the level of the I band, where they form two branched networks that surround the myofibrils on either side of the Z line (Fig. 1). As in other mammalian muscles, continuities within the network are quite extensive (Franzini-Armstrong, 2007), but it is also clear that frequent interruptions are present.

The average size of mitochondrial profiles differs between resting and exercised muscles, resulting in thinner profiles in the latter although the same overall disposition is maintained (Fig. 1A,B). The effect is quite noticeable by eye and it affects the entire mitochondrial network in all type IIB/IIX fibers examined. A quantitative estimate of the effect was obtained by measuring the width of mitochondrial profiles at a number of sites in a series of randomly collected images. The average mitochondrial width is significantly smaller in fatigued extensor digitorum longus (EDL) muscles than EDL at rest: $0.10 \pm 0.02 \mu\text{m}$ (mean \pm s.d.) vs $0.14 \pm 0.02 \mu\text{m}$ (Fig. 1C).

A second independent variation in exercised IIB/IIX muscle fibers is a significant increase in mitochondrial profiles involving unique elongated mitochondrial constrictions (EMCs) connecting two adjacent segments of the same mitochondrion (Fig. 2A–F). These constrictions are suggestive of intermediate steps in the fission process and are characterized by variable lengths, width and structure. Some EMCs constitute a tubular formation containing visible matrix and cristae (Fig. 2A–C); others are considerably narrower and are delimited by a double mitochondrial membrane and characterized by an empty or totally collapsed lumen (Fig. 2D–F). The overall occurrence of EMCs is low, with the frequency of mitochondrial constrictions noted in the entire sample of cross sections of random IIB/IIX fibers in resting muscle at 0.65 constrictions/fiber cross section (see Materials and Methods).

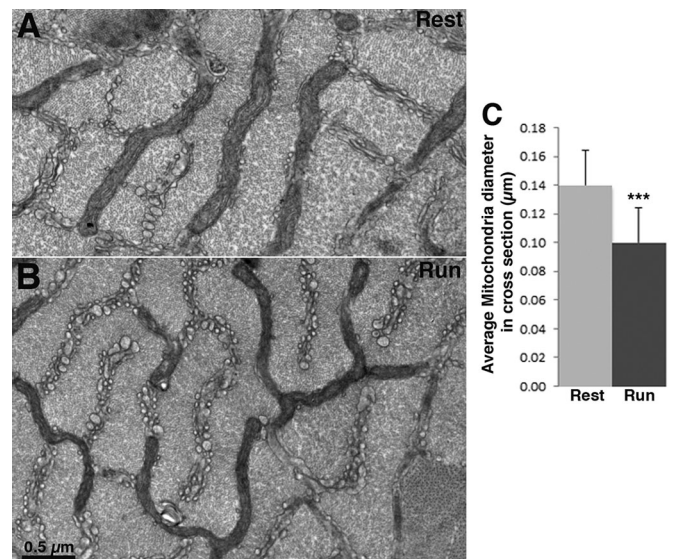


Fig. 1. Mitochondria are smaller in fast-twitch fibers of mice at the end of a run. (A,B) Cross section of IIB/IIX fibers at the level of the I band in EDL at rest and after mice run on a treadmill to the point of exhaustion. Mitochondria are located between myofibrils in two transverse planes on either side of the Z line. Mitochondria have the same overall distribution, but they are noticeably thinner in fibers of mice after treadmill exercise (B) than in fibers of mice at rest (A). (C) Mean \pm s.d. mitochondrial width measured at three spots for each mitochondrion at right angle to the long axis of the organelle is $0.10 \pm 0.02 \mu\text{m}$ in fibers from exercised mice (Run) ($n=251$ mitochondria, 20 cells, 41 images at $26,300\times$, 4 mice) and $0.14 \pm 0.02 \mu\text{m}$ in fibers from resting mice (Rest) ($n=190$ mitochondria, 23 cells, 40 areas at $26,300\times$, 4 mice); Student's *t*-test, *** $P<0.0001$.

However, in fibers from exercised muscles, although still relatively rare, EMCs are significantly more frequent: 2.80 constrictions/fiber cross section (Fig. 2G). This increase in EMCs was consistent across all muscles from the exercised group (Fig. 2H). In order to determine the relevance of these numbers, we obtained a rough count of the number of apparently individual mitochondrial profiles present in the same cross sections: ~ 50 profiles/fiber cross section. This indicates that even in exercised muscle, only $\sim 5\%$ of mitochondria were undergoing changes leading to constrictions at the time muscles were fixed, suggesting that the constrictions are rare and/or of short duration.

If EMCs are indicative of an intermediate step in mitochondrial fission, then some evidence should be found for successive stages. This is indeed the case; many of the elongated constriction sites evolve into very thin connecting necks (Fig. 2D–F). We call these structures 'mitochondria on a string' (MOAS), as suggested by Zhang et al. (2016) in the analysis of mitochondria in brain tissue. MOAS frequency is almost 40 times higher in fatigued versus resting fibers: 0.83 vs 0.022 MOAS/fiber (Fig. 2I). Comparison of Fig. 2G and Fig. 2I shows that about a third of the constrictions develop from the more variable shapes to the very thin ones. A final step is the actual fission of the mitochondrion into small fragments, with the loss of the extended elongated structures that characterize intermyofibrillar mitochondria in type IIB/IIX fibers. Exercised fibers show very little direct evidence for mitochondrial fragmentation, so constrictions do not necessarily lead to fission.

Overall mitochondrial diameter decreases and frequency of EMCs increases in electrically stimulated muscle

Fast-twitch fibers in electrically stimulated EDL show slightly but significantly thinner mitochondria compared to unstimulated EDL

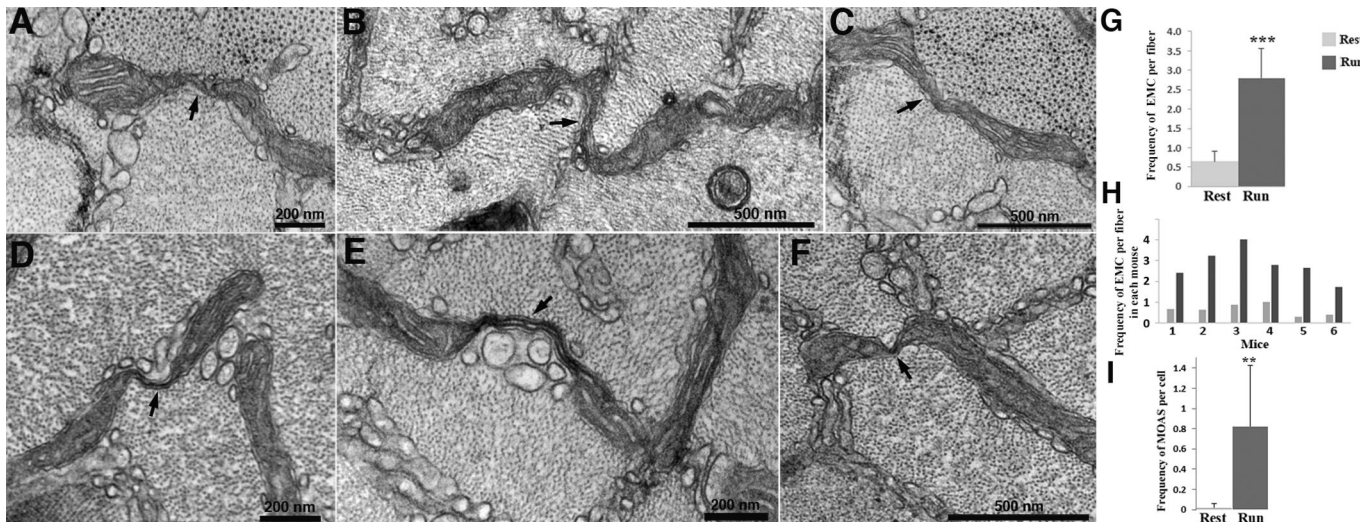


Fig. 2. Elongated mitochondrial constrictions (EMC) in fast-twitch fibers after fatigue. A close examination of the elongated mitochondria within the I band reveals sites at which the width of the organelle is abruptly decreased, resulting in a narrow neck (arrows) connecting two adjacent sections of the same mitochondrion. The extent and size of elongated constrictions are variable and their frequency depends on the muscle status, resting versus fatigued. All images shown are from fatigued muscles. (A–C) Intermediate stages where the matrix and cristae are visible in the constricted region. (D–F) Extreme cases of elongated constrictions, most likely the last stage of the fission process, where the very thin neck is composed only of the double mitochondrial membrane. Mitochondria connected by these extreme constrictions are called ‘mitochondria on a string’ (MOAS, from Zhang et al., 2016). (G). Mean±s.d. EMC frequency/fiber is significantly higher in mice after a run compared to mice at rest: 2.80 ± 0.77 ($n=6$ mice, 53 fibers) vs 0.65 ± 0.27 ($n=6$ mice, 58 fibers). (H) Mean frequency of EMC in fibers from individual mice at rest and after running. (I) Mean±s.d. MOAS frequency is significantly higher in EDL from mice after a run than in EDL from mice at rest: 0.83 ± 0.60 ($n=6$ mice, 53 fibers) vs 0.02 ± 0.04 , ($n=6$ mice, 58 fibers). Student's *t*-test, ** $P < 0.01$, *** $P < 0.001$.

with measured widths of 0.11 ± 0.02 (160 mitochondria, 15 cells, 3 mice) vs 0.14 ± 0.03 μm (146 mitochondria, 15 cells, 3 mice; mean±s.d., *t*-test, $P < 0.0001$). Stimulated EDL fibers also display a significant increase in frequency of mitochondrial constrictions (Fig. 3A–E) involving the same variety of changes from partial to intense constrictions as observed in exercised fibers (compare with Fig. 2A–F). The frequency of elongated mitochondrial constrictions in the stimulated vs resting EDL is 2.1 vs 0.94 EMCs/fiber in cross section (Fig. 3F). The frequencies are essentially similar to those observed in muscles after exercise (see section above and Fig. 2G). However there is no significant incidence of the extreme case of

multiple constrictions creating a MOAS effect. In stimulated muscles small mitochondrial clusters and mitochondria with a round rather than elongated profile are observed, suggesting an ongoing process of fragmentation (Fig. 3D,E). However, this effect is not frequent and, as indicated above, this is not obvious in muscles after exercise.

Drp1 recruitment to the mitochondrial membrane is affected by exercise and electrical stimulation

To investigate the molecular mechanism behind the formation of EMCs, we evaluated the expression and phosphorylation of a key

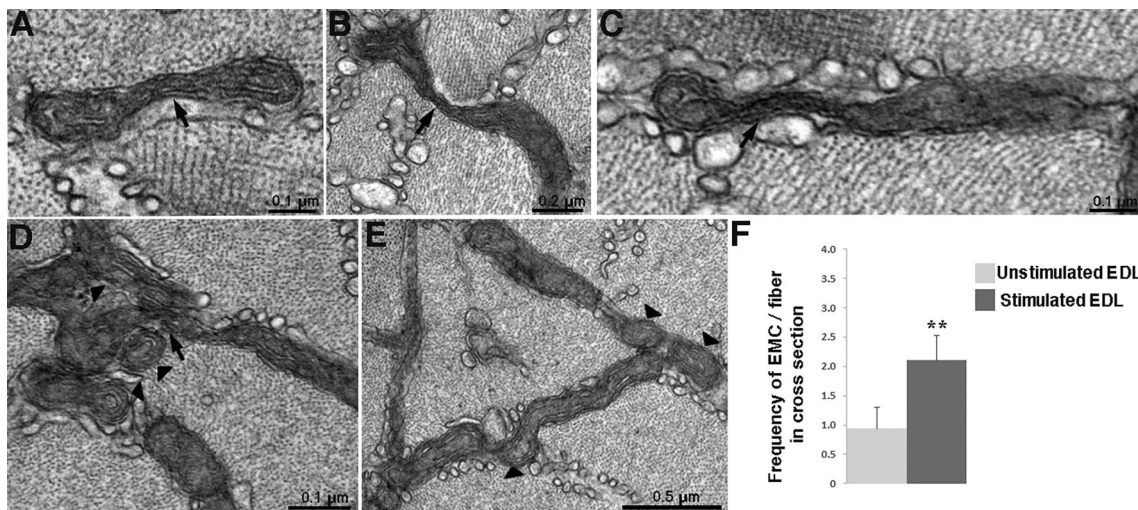


Fig. 3. Elongated mitochondrial constrictions in fatigue induced by electrical stimulation. (A–C) Cross sections of fibers from electrically stimulated muscles demonstrate the presence of elongated mitochondrial constrictions (EMCs) (arrows). (D) The presence of EMCs (arrows) is sometimes accompanied by clusters of rounded small mitochondrial profiles (arrowheads), which may originate from fission events. (E) Round profiles appearing at the end of mitochondria are indicative of fragmentation (arrowhead). (F) The mean±s.d. frequency of EMCs is significantly higher in electrically stimulated EDLs than in unstimulated ones: 2.10 ± 0.42 ($n=45$ fibers, 4 mice,) vs 0.94 ± 0.36 EMCs/fiber ($n=42$ fibers, 4 mice). Student's *t*-test, ** $P < 0.01$.

fission protein: dynamin-related protein 1 (Drp1), in exercised muscle and electrically stimulated muscles. Phosphorylation of Drp1 at Ser 616 promotes translocation of Drp1 to the mitochondria, facilitating mitochondrial fission (Taguchi et al., 2007). Levels of p-Drp1 (Ser 616) are increased in EDL after treadmill exercise (Fig. 4A). The pixel density ratio of p-Drp1 (Ser 616) to total Drp1 is increased by ~8-fold: 0.071 at rest vs 0.60 after exercise (Fig. 4B), suggesting an increased recruitment of Drp1 to the mitochondrial membrane. After electrical stimulation, tibialis anterior (TA) muscles show a slightly more modest ~4-fold increase in the ratio of p-Drp1 (Ser 616) to total Drp1: 0.98 unstimulated vs 4.18 stimulated (Fig. 4D).

Levels of total Drp1 are slightly, but not significantly, increased in muscles after exercise but not after electrical stimulation. This situation can be explained by the two experiments, physical exercise and electrical stimulation, involving different physiological conditions. To prepare mice to run on treadmill, they are first acclimated for one week and then subjected to running for up to one hour, whereas the mice in the electrical stimulation group were not prepared. Additionally the electrical stimulation is over a shorter period of 30 min and involves less overall energy consumption and thus possibly less anoxia than exercise.

Possible involvement of sarcoplasmic reticulum in the development of mitochondrial constrictions

We observe a specific, potentially relevant interaction between SR and mitochondria at sites of constrictions; SR fingers are frequently closely opposed to constricted sites and seem to push into them (Fig. 5). A wedge may appear to be inserted in the elongated neck region (Fig. 5A–C), or an elongated finger closely encircles a constricted mitochondrial segment forming a ring around it (Fig. 5G–I). In the area of contact between the SR and mitochondrial membrane, electron-dense areas are seen (Fig. 5D–F). SR closely opposed to the EMCs is observed in all conditions at a percentage frequency (closely associated SR/EMCs \times 100) of: 16% in resting, 31% in run, and 26% in unstimulated control, 28% in stimulated muscles.

DISCUSSION

Our imaging data show that acute exercise and electrical muscle stimulation induce an increase in intermediate and advanced stages of mitochondrial stress-dependent events, possibly leading to fission in fast-twitch and/or fatigable fibers. The noticeable effect is the formation of unusual mitochondrial profiles with elongated constrictions (EMCs) that constitute a novel direct view of the process. Constrictions are rare in resting muscle and thus had so far escaped attention and obviously have been missed in past studies of fatigued muscle. Most of the constrictions that we observe are of short length and they may be of brief duration in line with the highly dynamic responses of mitochondria. However, it is conceivable that if similar constrictions are long-lived, they may develop into the very thin elongated connections between mitochondria observed in brain tissue of mice carrying human familial Alzheimer's disease (FAD) mutations (Zhang et al., 2016), and in some not well-defined conditions of human pathology (Vincent et al., 2016).

If mitochondria undergo fission, the obvious question is whether this fission results in the appearance of small mitochondrial profiles deriving from fragmentation of the normal elongated mitochondria. Mitochondrial fragmentation, resulting in the accumulation of smaller organelles, is easily detected in conditions of energetic stress and unbalanced Ca^{2+} homeostasis (Wu et al., 2010; Iqbal and Hood, 2014; Lavorato et al., 2015). However, despite evidence for possible mitochondrial fission events, we find very little obvious evidence for fragmented mitochondria after electrical stimulation and practically no evidence after treadmill exercise. This may be in part owing to the fact that only a minor portion (~5%) of mitochondria show evidence for actual fission at one time. Gollnick and King (1969) have reported an apparent increase in the frequency of mitochondrial profiles in exercised rat muscle, but have not demonstrated any direct evidence for their origin. More importantly, either the fission process in fatigued muscles is slow, or the increase in Drp1 may be related more to activation of respiration (Wei et al., 2011; Zhang et al., 2017) than to actual fission. It is reassuring that fatigue induced under functional conditions similar to those encountered by humans performing endurance exercise (primarily

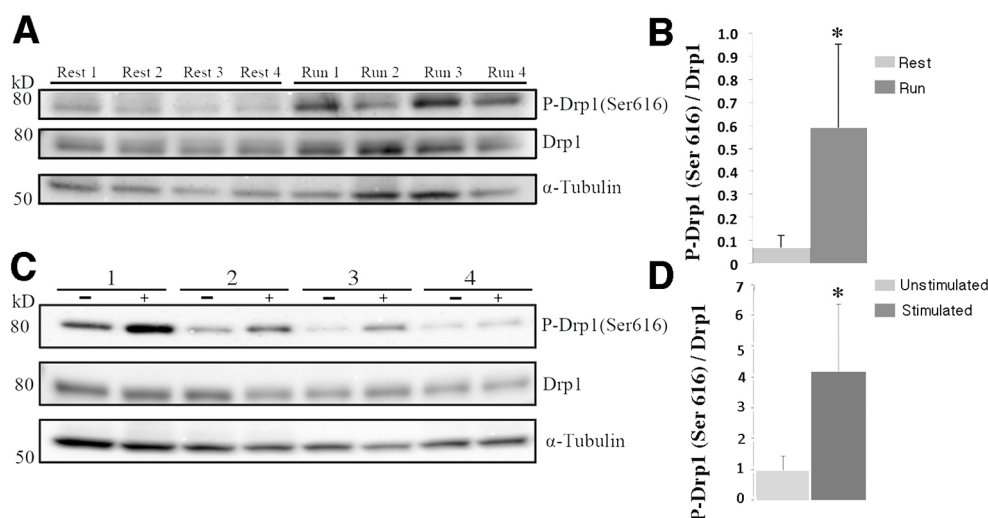


Fig. 4. Increased p-Drp1 (Ser 616) levels in mitochondria of exercised and electrically stimulated muscles. (A,C) Immunoblot analysis of p-Drp1 (Ser 616) and total Drp1 in EDL from mice at rest and after running ($n=4$ mice each) (A), and TA from mice in the unstimulated and electrically stimulated groups ($n=4$ mice each) (C). In C, 1–4 indicates the number of mice used. (B,D) Mean \pm s.d. pixel density ratio of p-Drp1 (Ser 616) to total Drp1 (normalized to α -tubulin) is 8-fold higher in EDL from mice after exercise compared to the muscles from resting mice (0.60 ± 0.36 vs 0.071 ± 0.05) (B), and 4.3-fold higher in electrically stimulated TA than in unstimulated TA (4.18 ± 4.35 vs 0.98 ± 0.93 , paired t -test, $*P<0.05$) (D). The densitometric ratio of p-Drp1 (Ser 616) to α -tubulin is also higher in run versus control (mean \pm s.d., 0.005 ± 0.003 vs 0.0008 ± 0.0008 , $P<0.05$) and in stimulated versus contralateral leg (1.31 ± 1.77 vs 0.42 ± 0.30 , $P=0.09$, paired t -test) (data not shown).

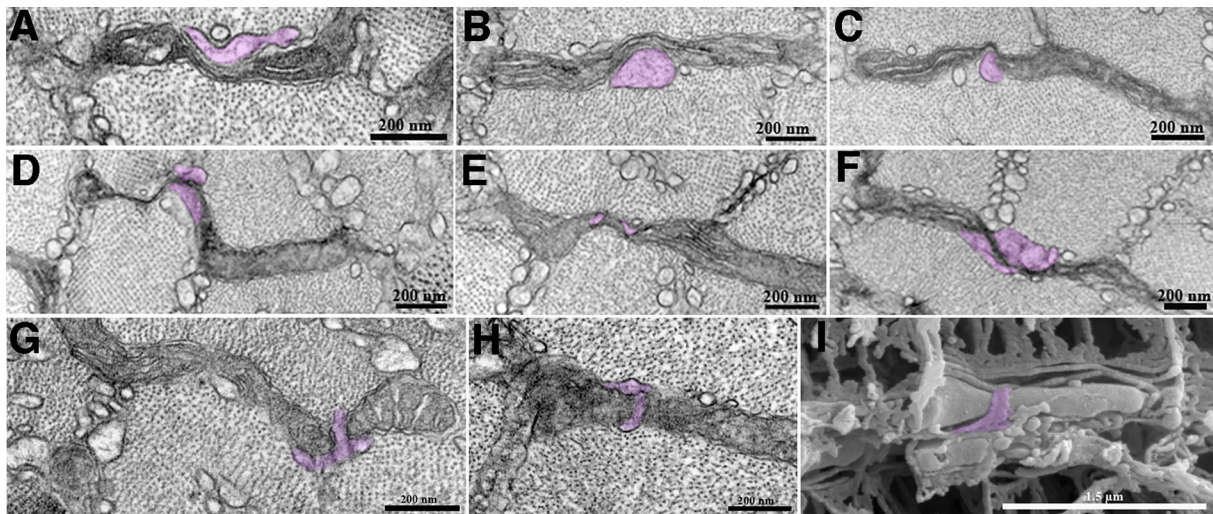


Fig. 5. Mitochondrial constrictions and sarcoplasmic reticulum. The sarcoplasmic reticulum (SR, purple) is often closely associated with mitochondrial constrictions, either forming a sort of wedge (A–C) or wrapping around mitochondria, especially around the neck of the organelle at sites of constriction (D–H). These structures were also observed using three-dimensional scanning electron microscopy (I).

an oxygen-dependent form of exercise such as long-distance running) has a definite effect on mitochondria but does not result in massive fragmentation.

Considering that Drp1 activation via Ser 616 phosphorylation (Taguchi et al., 2007) is related to mitochondrial fission and that Ser 616 phosphorylation is observed in muscle affected by acute exercise or stimulation, it is likely that the observed increase in EMCs results from an increase in Drp1 recruitment to the mitochondrial membrane, which induces incipient fission. However, the process of fission is apparently somewhat slowed down or arrested in intermediate stages. Indeed, an increase in mitochondrial constriction frequency has previously been associated with increased levels of p-Drp1 (Ser 616) and with a delay in fission process in an Alzheimer's disease model (Zhang et al., 2016).

Several factors may explain the small differences observed between fatigue induced by extensive exercise and by direct muscle stimulation. First, the duration of the electrical stimulation protocol was shorter: 30 min vs 45–60 min. Secondly, oxygen consumption and thus hypoxia are probably considerably less in the electrical stimulation, which involves only the leg muscles, whereas most of the body muscles are involved during physical exercise. Thus low oxygen stress may be a contributing factor in the stimulation of mitochondrial fission. Additionally, mice subjected to treadmill exercise were acclimated for one week, which may affect mitochondrial biogenesis and synthesis of mitochondrial proteins such as Drp1, increasing its levels at rest and affecting its response to the running exercise stimulus.

Using both 2D and 3D microscopy, we observed that the sarcoplasmic reticulum may be closely opposed to the sites where mitochondria are thinned and extended (EMCs) in a manner highly suggestive of a role in inducing constrictions. A role for the ER in initiating mitochondrial fission has been proposed on the basis of light microscope observations (Friedman et al., 2011) but not demonstrated at higher resolution. We clearly detect the formation of SR wedges at sites of incipient mitochondrial constrictions, thus providing a new insight into the relationship between SR and mitochondria in the fission process. The SR may facilitate the sharp change in membrane curvature that occurs at sites of EMCs.

It is not clear how the small but significant decrease in mitochondrial volume, detected as a small change in their diameter, is related to the constriction events. Since the latter are

fairly rare while the former affects the entire network, the two may not be related.

MATERIALS AND METHODS

Experimental animals

All animal experiments were in accordance with protocols approved by the Institutional Animal Care and Use Committee (IACUC) of Thomas Jefferson University and University of Pennsylvania. For treadmill experiments, 7–8-month-old C57BL/6 mice were maintained at the Animal Core Facility of the Department of Pathology, Anatomy and Cell Biology, Thomas Jefferson University, accredited by AAALAC. For *in vivo* muscle stimulation, 5–6-month-old C57BL/6 mice were used. Mice were housed at 22°C under a 12-h light/12-h dark cycle with food and water provided *ad libitum*.

Treadmill exercise

7–8-month-old C57BL/6 mice were subjected to exercise on a treadmill equipped with an electrical shock grid. Mice were previously acclimated for one week with a single 30 min run per day, with gradual increase of velocity up to 20 m/min. For the test, mice were subjected to runs starting at a velocity of 10 m/min, increasing by 2 m/min every 2 min up to a maximum of 20 m/min. No mouse responded to repeated prodding at the end of one hour running exercise on the treadmill, with some mice failing to respond after 45 min. Mice that faltered before the 45 min period were not included in the subsequent analysis. Euthanasia by cervical dislocation was immediate at the end of the exercise and extensor digitorum longus (EDL) muscles were harvested within minutes and processed for electron microscopy (EM) and for immunoblot analysis. Resting mice were used as controls.

Simulation of high-intensity exercise using electrical muscle stimulation

An *in vivo* sciatic nerve muscle stimulation protocol was developed in order to simulate the exercise of mice on treadmill. One leg of each mouse was stimulated, while the other leg was used as unstimulated control. Mice were anesthetized with 1–2% of isoflurane. Depth of anesthesia was confirmed through toe pinch and monitoring the heart rate with a pulse oximeter. The sciatic nerve was exposed and connected to a custom-made bipolar stimulating electrode driven by a Grass S48 stimulator. Two recording silver EMG needle electrodes were applied, one in the gastrocnemius and the other near the Achilles tendon. The ground electrode was connected to the skin of the back of the mouse. The recording electrodes were then connected to a Warner Instruments DP-311 differential amplifier and finally to an A/D converter. The EMG signal was used as a measure of fatigue. Muscles were

collected immediately at the end of the stimulation: the EDL was used for EM and tibialis anterior (TA) for western blot analysis. Both muscles have a high content of fast-twitch fibers.

To design the stimulation protocol, mice running on the treadmill at 20 m/min were video recorded in order to visualize the stepping frequency. A back foot stepping frequency of 6 Hz was observed, consistent with fast limb movements recorded in freely running mice (Bellardita and Kiehn, 2015). We designed a stimulation protocol that would subject the hind leg muscles to an exercise load equivalent to treadmill running. First, we observed that during 30 min experiments the mice run intermittently with short periods of inactivity. Based on this behavior, our maximal protocol consisted of stimulation bursts lasting 10 s, followed by 10 s of inactivity. This 10 s on–10 s off burst protocol lasted 30 min (Fig. 6). Secondly, we matched the stimulation pattern to that of a fast-running posterior leg. Each 10 s burst consisted of trains of 5 V stimuli each lasting 0.1 s at a frequency of 100 Hz, the normal frequency of fast fibers recorded *in vivo* (Hennig and Lomo, 1985) (Fig. 6C). Each train was repeated at the same frequency as the stepping (6 Hz), with short intervals between, mimicking the pushing and retreating pattern of the hind foot. (Fig. 6B). Evoked action potentials were recorded through the stimulation. The high-intensity stimulation caused an 80% decrease in EMG amplitude within the first 5 min and a decline at each stimulus (Fig. 6A,B), possibly related to depletion of glycogen and phosphocreatine (Katz et al., 2003). Response decline within the following 25 min of stimulation was minor. The stimulation protocol induced the phosphorylation of known exercise-sensitive proteins such as p70/85S6K, AMPK, ERK (Potts et al., 2017; Hoffman et al., 2015) compared to non-stimulated sham control animal (sham –), non-stimulated sham control animal after 30 min (sham +), and the contralateral non-stimulated leg of the same animal (stim –) (Fig. 6F).

Thin-section electron microscopy

EDL muscles were dissected, pinned down at approximately resting length, fixed by means of immersion in 6% (vol/vol) glutaraldehyde in 0.1 M sodium

cacodylate buffer (pH 7.4) at room temperature and further processed for standard thin-section electron microscopy as in Lavorato et al. (2017). The embedded muscles were carefully mounted, so precisely oriented cross and longitudinal sections were routinely obtained (see Fig. S1).

Thin-section electron microscopy quantification

Electron microscopy and subsequent analysis were performed on cross sections of muscles. Observations were limited to fast-twitch fatigable fiber types IIB and IIX. Mouse EDL contains approximately 70–75% type IIB, 10–15% IIX, 8% IIA and 4% I muscle fibers (Hughes et al., 1999; Danieli-Betto et al., 2005). Type IIB and IIX fibers are easily distinguishable from the others by the fact that mitochondria are limited to the I bands and that clusters at fiber edges are not present. However, distinction between type IIB and IIX fibers is not obvious and so it was not attempted (Boncompagni et al., 2010). Mitochondrial width was measured at several points along each profile in randomly selected EM images from muscle cross sections at a magnification of 26,300 \times using Fiji program (NIH). The frequency of mitochondria showing elongated constrictions was very low, so quantitation required large sample sizes. We obtained well-oriented cross sections of large muscle bundles, each showing up to 50 fiber profiles. All IIB/IIX fiber profiles that appeared entirely in the section and were not hindered by the thin grid bars were accepted for counting (Fig. S1). As the fast fibers are fairly uniform in diameter, the cross sectional area was used as a reference. Elongated constrictions were visually identified and their numbers counted in each fiber cross section. The numbers, expressed as number of profiles/fiber cross section are proportional to the constriction frequencies in the fiber volume.

Scanning electron microscopy

EDL muscles were fixed in 0.5% paraformaldehyde and 1.0% glutaraldehyde at room temperature for a minimum of 30 min, cryoprotected in 40% glycerol, frozen in propane, cryofractured and macerated through prolonged exposure

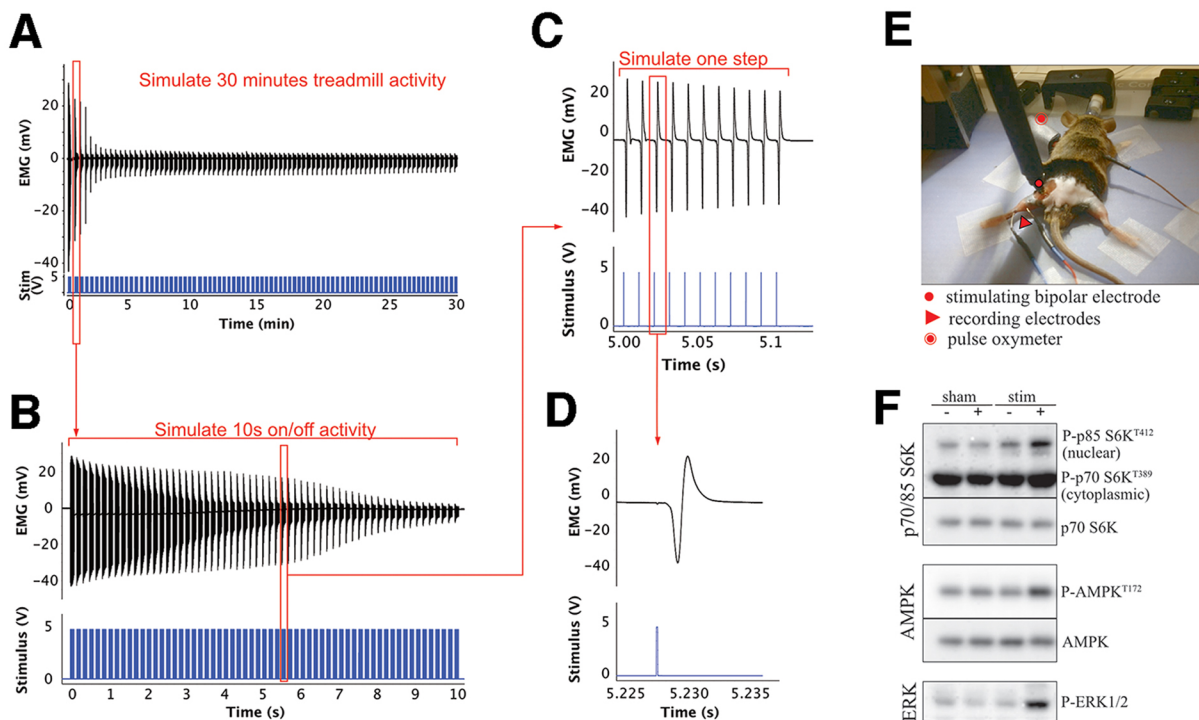


Fig. 6. Sciatic nerve high-intensity stimulation protocol. (A,B) Electromyographic (EMG) and stimulus traces over 30 min of intermittent (10 s on/10 s off) sciatic stimulation that mimics the frequently interrupted running activity of mice (see Materials and Methods). (A) Each stimulus trace (in blue) represents a burst of 10 s (shown in detail in B). The EMG amplitude, relating the muscle response, shows an ~80% decrease in amplitude within the first 5 min and a small decline after that. (B) A detail of a single burst of 5 V stimuli at 100 Hz repeated at 6 bursts/s, showing the response decline within one of the initial bursts. (C) Enlarged representation of a few of the evoked muscle action potentials repeated at 100 Hz for 100 ms in each burst. (D) Single muscle action potential evoked on stimulation of the sciatic nerve with a 5 V stimulus. (E) Stimulating and recording electrode placement. (F) Immunoblotting analysis reveals that stimulation of muscles induces increased phosphorylation of known exercise-sensitive proteins such as p70/85S6K, AMPK and ERK.

to low concentration (~0.1%) OsO₄ for 48–72 h, critical point dried, sputter-coated for conductivity and observed using a FEI Quanta 250 scanning electron microscope. The technique was developed by Tanaka and Mitsuhashi (1984) and effectively used by Ogata and Yamasaki (1990), see also Ogata and Yamasaki (1993) for a review.

Western blot analysis

EDL and TA muscles were homogenized and subjected to SDS-PAGE followed by immunoblot analysis, as previously described (Loro et al., 2015). Antibodies raised against the following were used: phospho p70/S6 kinase (Cell Signaling Technology, clone 1A5, 9206; 1:2000), p70 S6 Kinase (Cell Signaling Technology, clone 49D7, 2708; 1:2000), phospho AMPK T172 (Cell Signaling Technology, clone 40H9, 2535; 1:2000), AMPK (Cell Signaling Technology, clone D5A2, 5831; 1:2000), active MAPK (p-ERK1/2) (Promega, V8031; 1:5000), DRP1 (BD Biosciences, clone 8/DRP1, 61113; 1:1000), phospho DRP1 S616 (Cell Signaling Technology, 3455; 1:2000), α tubulin (Sigma-Aldrich, T6199; 1:5000). Digital images of the plots were scanned using Fiji program (ImageJ, NIH) to obtain pixel density of bands. The total pixel density for each band, normalized to α tubulin, was used for the purpose of comparing protein amounts.

Acknowledgements

We thank Dr Stephen Hollingworth for constructive suggestions.

Competing interests

The authors declare no competing or financial interests.

Author contributions

Conceptualization: M.L., C.F.-A.; Methodology: M.L., E.L., V.D.; Validation: E.L.; Formal analysis: M.L.; Investigation: M.L., E.L.; Resources: V.D.; Data curation: M.L.; Writing - original draft: M.L., C.F.-A.; Writing - review & editing: M.L., E.L., T.S.K., C.F.-A.; Supervision: M.L., C.F.-A.; Funding acquisition: C.F.-A.

Funding

Supported by National Institute of Arthritis and Musculoskeletal and Skin Diseases (NIAMS) [grant AR 052354-06A1, P.I. P. D. Allen, St James's University Hospital, Leeds, UK (to C.F.-A.)]; and ITMAT grant, National Center for Advancing Translational Sciences of the National Institutes of Health [award UL1TR000003 to T.S.K.]. Deposited in PMC for release after 12 months.

Supplementary information

Supplementary information available online at <http://jcs.biologists.org/lookup/doi/10.1242/jcs.221028.supplemental>

References

- Allen, D. G. and Westerblad, H. (2001). Role of phosphate and calcium stores in muscle fatigue. *J. Physiol.* **536**, 657–665.
- Bangsbo, J. (2000). Muscle oxygen uptake in humans at onset of and during intense exercise. *Acta Physiol. Scand.* **168**, 457–464.
- Bellardita, C. and Kiehn, O. (2015). Phenotypic characterization of speed-associated gait changes in mice reveals modular organization of locomotor networks. *Curr. Biol.* **25**, 1426–1436.
- Boncompagni, S., Loy, R. E., Dirksen, R. T. and Franzini-Armstrong, C. (2010). The I4895T mutation in the type 1 ryanodine receptor induces fiber-type specific alterations in skeletal muscle that mimic premature aging. *Aging Cell* **9**, 958–970.
- Boncompagni, S., Rossi, A. E., Micaroni, M., Bezoussenko, G. V., Polishchuk, R. S., Dirksen, R. T. and Protasi, F. (2009a). Mitochondria are linked to calcium stores in striated muscle by developmentally regulated tethering structures. *Mol. Biol. Cell.* **20**, 1058–1067.
- Boncompagni, S., Rossi, A. E., Micaroni, M., Hamilton, S. L., Dirksen, R. T., Franzini-Armstrong, C. and Protasi, F. (2009b). Characterization and temporal development of cores in a mouse model of malignant hyperthermia. *Proc. Natl. Acad. Sci. USA* **106**, 21996–22001.
- Chan, D. C. (2012). Fusion and fission: interlinked processes critical for mitochondrial health. *Annu. Rev. Genet.* **46**, 265–287.
- Chen, H. and Chan, D. C. (2010). Physiological functions of mitochondrial fusion. *Ann. N. Y. Acad. Sci.* **1201**, 21–25.
- Cheng, A. J., Yamada, T., Rassier, D. E., Andersson, D. C., Westerblad, H. and Lanner, J. T. (2016). Reactive oxygen/nitrogen species and contractile function in skeletal muscle during fatigue and recovery. *J. Physiol.* **594**, 5149–5160.
- Coronado, M., Fajardo, G., Nguyen, K., Zhao, M., Kooiker, K., Jung, G., Hu, D.-Q., Reddy, S., Sandoval, E., Stotland, A. et al. (2018). Physiological mitochondrial fragmentation is a normal cardiac adaptation to increased energy demand. *Circ. Res.* **122**, 282–295.
- Dahl, R., Larsen, S., Dohmann, T. L., Qvortrup, K., Helge, J. W., Dela, F. and Prats, C. (2015). Three-dimensional reconstruction of the human skeletal muscle mitochondrial network as a tool to assess mitochondrial content and structural organization. *Acta Physiol. (Oxf.)* **213**, 145–155.
- Danielli-Betto, D., Esposito, A., Germinario, E., Sandonà, D., Martinello, T., Jakubiec-Puka, A., Biral, D. and Betto, R. (2005). Deficiency of alpha-sarcoglycan differently affects fast- and slow-twitch skeletal muscles. *Am. J. Physiol. Regul. Integr. Comp. Physiol.* **289**, R1328–R1337.
- Fitt, R. H. (1994). Cellular mechanisms of muscle fatigue. *Physiol. Rev.* **74**, 49–94.
- Franzini-Armstrong, C. (2007). ER-mitochondria communication. How privileged? *Physiology* **22**, 261–268.
- Franzini-Armstrong, C. and Boncompagni, S. (2011). The evolution of the mitochondria-to-calcium release units relationship in vertebrate skeletal muscles. *J. Biomed. Biotech.* **2011**, 830573.
- Friedman, J. R., Lackner, L. L., West, M., DiBenedetto, J. R., Nunnari, J. and Voeltz, G. K. (2011). ER tubules mark sites of mitochondrial division. *Science* **334**, 358–362.
- Glancy, B., Hartnell, L. M., Malide, D., Yu, Z.-X., Combs, C. A., Connelly, P. S., Subramaniam, S. and Balaban, R. S. (2015). Mitochondrial reticulum for cellular energy distribution in muscle. *Nature* **523**, 617–620.
- Gollnick, P. D. and King, D. W. (1969). Effect of exercise and training on mitochondria of rat skeletal muscle. *Am. J. Physiol.* **216**, 1502–1509.
- Henning, R. and Lomo, T. (1985). Firing patterns of motor units in normal rats. *Nature* **314**, 164–166.
- Hoffman, N. J., Parker, B. L., Chaudhuri, R., Fisher-Wellman, K. H., Kleinert, M., Humphrey, S. J., Yang, P., Holliday, M., Trefely, S., Fazakerley, D. J. et al. (2015). Global phosphoproteomic analysis of human skeletal muscle reveals a network of exercise-regulated kinases and AMPK substrates. *Cell. Metab.* **22**, 922–935.
- Hughes, S. M., Chi, M. M.-Y., Lowry, O. H. and Gundersen, K. (1999). Myogenin induces a shift of enzyme activity from glycolytic to oxidative metabolism in muscles of transgenic mice. *J. Cell. Biol.* **145**, 633–642.
- Iqbal, S. and Hood, D. A. (2014). Oxidative stress-induced mitochondrial fragmentation and movement in skeletal muscle myoblasts. *Am. J. Physiol. Cell Physiol.* **306**, C1176–C1183.
- Kamandulis, S., de Souza Leite, F., Hernández, A., Katz, A., Brazaitis, M., Bruton, J. D., Venckunas, T., Masiulis, N., Mickeviciene, D., Eimantas, N. et al. (2017). Prolonged force depression after mechanically demanding contractions is largely independent of Ca²⁺ and reactive oxygen species. *ASEB J.* **31**, 4809–4820.
- Katz, A., Andersson, D. C., Yu, J., Norman, B., Sandström, M. E., Wieringa, B. and Westerblad, H. (2003). Contraction-mediated glycogenolysis in mouse skeletal muscle lacking creatine kinase: the role of phosphorylase b activation. *J. Physiol.* **555**, 523–531.
- Lavorato, M., Huang, T.-Q., Iyer, V. R., Perni, S., Meissner, G. and Franzini-Armstrong, C. (2015). Dyad content is reduced in cardiac myocytes of mice with impaired calmodulin regulation of RyR2. *J. Muscle Res. Cell. Motil.* **36**, 205–214.
- Lavorato, M., Gupta, P. K., Hopkins, P. M. and Franzini-Armstrong, C. (2016). Skeletal muscle microalterations in patients carrying Malignant Hyperthermia-related mutations of the e-c coupling machinery. *Eur. J. Transl. Myol.* **26**, 6105.
- Lavorato, M., Iyer, V. R., Dewight, W., Cupo, R. R., Debattisti, V., Gomez, L., De la Fuente, S., Zhao, Y.-T., Valdivia, H. H., Hajnóczky, G. et al. (2017). Increased mitochondrial nanotunneling activity, induced by calcium imbalance, affects intermitochondrial matrix exchanges. *Proc. Natl. Acad. Sci. USA* **114**, E849–E858.
- Loro, E., Seifert, E. L., Moffat, C., Romero, F., Mishra, M. K., Sun, Z., Krajacic, P., Anokye-Danso, F., Summer, R. S., Ahima, R. S. et al. (2015). IL-15R α is a determinant of muscle fuel utilization, and its loss protects against obesity. *Am. J. Physiol. Regul. Integr. Comp. Physiol.* **309**, R835–R844.
- Mannella, C. A., Buttler, K., Rath, B. K. and Marko, M. (1998). Electron microscopic tomography of rat-liver mitochondria and their interactions with the endoplasmic reticulum. *Biofactors* **8**, 225–228.
- Nagasser, A. S., van der Laarse, W. J. and Elzinga, G. (1992). Metabolic changes with fatigue in different types of single muscle fibers of *Xenopus laevis*. *J. Physiol.* **448**, 511–523.
- Nassar-Gentina, V., Passonneau, J. V. and Rapoport, S. I. (1981). Fatigue and metabolism of frog muscle fibers during stimulation and in response to caffeine. *Am. J. Physiol.* **241**, C160–C166.
- Ogata, T. and Yamasaki, Y. (1990). High-resolution scanning electron microscopic studies on the three-dimensional structure of the transverse-axial tubular system, sarcoplasmic reticulum and intercalated disc of the rat myocardium. *Anat. Rec.* **228**, 277–287.
- Ogata, T. and Yamasaki, Y. (1993). Ultra-high resolution scanning electron microscopic studies on the sarcoplasmic reticulum and mitochondria in various muscles: a review. *Scan. Microsc.* **7**, 145–156.
- Picard, M., Gentil, B. J., McManus, M. J., White, K., St. Louis, K., Gartside, S. E., Wallace, D. C. and Turnbull, D. M. (2013). Acute exercise remodels mitochondrial membrane interactions in mouse skeletal muscle. *J. Appl. Physiol.* **115**, 1562–1571.

- Potts, G. K., McNally, R. M., Blanco, R., You, J.-S., Hebert, A. S., Westphall, M. S., Coon, J. J. and Hornberger, T. A. (2017). A map of the phosphoproteomic alterations that occur after a bout of maximal-intensity contractions. *J. Physiol.* **595**, 5209-5226.
- Rana, A., Oliveira, M. P., Khamoui, A. V., Aparicio, R., Rera, M., Rossiter, H. B. and Walker, D. W. (2017). Promoting Drp1-mediated mitochondrial fission in midlife prolongs healthy lifespan of *Drosophila melanogaster*. *Nat. Commun.* **8**, 448-451.
- Taguchi, N., Ishihara, N., Jofuku, A., Oka, T. and Mihara, K. (2007). Mitotic phosphorylation of dynamin-related GTPase Drp1 participates in mitochondrial fission. *J. Biol. Chem.* **282**, 11521-11529.
- Tanaka, K. and Mitsushima, A. (1984). A preparation method for observing intracellular structures by scanning electron microscopy. *J. Microsc.* **133**, 213-222.
- Tinel, H., Cancela, J. M., Mogami, H., Gerasimenko, J. V., Gerasimenko, O. V., Tepikin, A. V. and Petersen, O. H. (1999). Active mitochondria surrounding the pancreatic acinar granule region prevent spreading of inositol trisphosphate-evoked local cytosolic Ca^{2+} signals. *EMBO J.* **18**, 4999-5008.
- Vincent, A. E., Ng, Y. S., White, K., Davey, T., Mannella, C., Falkous, G., Feeney, C., Schaefer, A. M., McFarland, R., Gorman, G. S. et al. (2016). The spectrum of mitochondrial ultrastructural defects in mitochondrial myopathy. *Sci. Rep.* **6**, 30610-30622.
- Wei, L., Salahura, G., Boncompagni, S., Kasischke, K. A., Protasi, F., Sheu, S.-S. and Dirksen, R. T. (2011). Mitochondrial superoxide flashes: metabolic biomarkers of skeletal muscle activity and disease. *FASEB J.* **25**, 3068-3078.
- Westerblad, H. and Allen, D. G. (1992). Myoplasmic free Mg^{2+} concentration during repetitive stimulation of single fibres from mouse skeletal muscle. *J. Physiol.* **453**, 413-434.
- Westerblad, H. and Allen, D. G. (1993). The influence of intracellular pH on contraction, relaxation and $[\text{Ca}^{2+}]_i$ in intact single fibres from mouse muscle. *J. Physiol.* **466**, 611-628.
- Westermann, B. (2010). Mitochondrial fusion and fission in cell life and death. *Nat. Rev. Mol. Cell. Biol.* **11**, 872-884.
- Wu, S., Zhou, F., Zhang, Z. and Xing, D. (2010). Mitochondrial oxidative stress causes mitochondrial fragmentation via differential modulation of mitochondrial fission-fusion proteins. *FEBS J.* **278**, 941-954.
- Zhang, L., Trushin, S., Christensen, T. A., Bachmeier, B. V., Gateno, B., Schroeder, A., Yao, J., Itoh, K., Sesaki, H., Poon, W. W. et al. (2016). Altered brain energetics induces mitochondrial fission arrest in Alzheimer's Disease. *Sci. Rep.* **6**, 18725.
- Zhang, H., Wang, P., Bisetto, S., Yoon, Y., Chen, Q., Sheu, S.-S. and Wang, W. (2017). A novel fission-independent role of dynamin-related protein 1 in cardiac mitochondrial respiration. *Cardiovasc. Res.* **113**, 160-170.

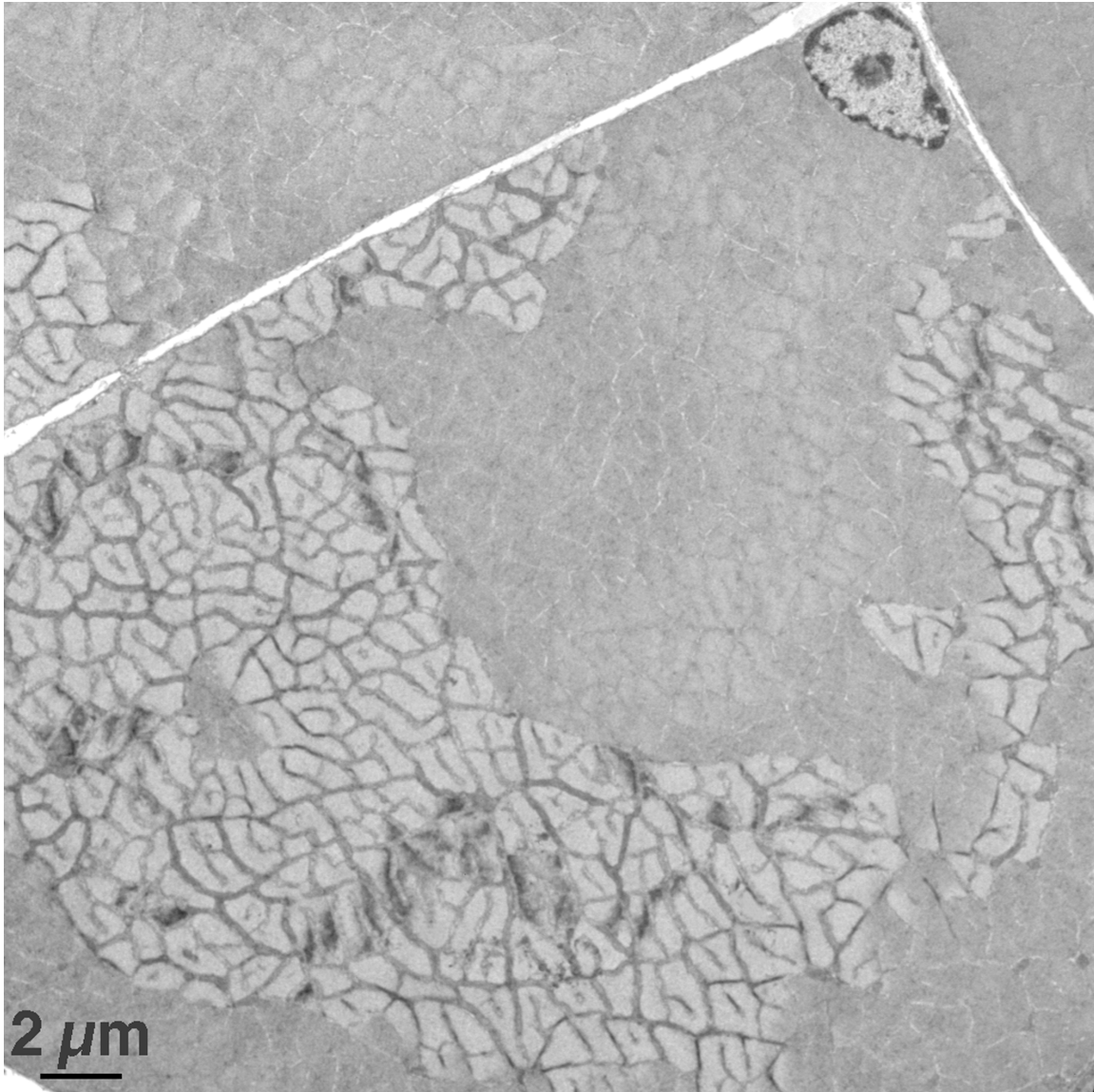


Figure S1. Low magnification image illustrating the standard quality of preservation and orientation of the images that were used to collect the data. Each cross sectional view had excellent presentations of I- and A- band areas and only images that covered entire fiber cross sections were employed for counts. The I-band areas were used for obtaining counts of the frequency of mitochondria with constrictions of the type illustrated in Figs. 2-4. A large sample (> 40 fibers each for rest and fatigued muscles) assured sufficient statistical reliability.